50TH EASTERN SNOW CONFERENCE
61ST WESTERN SNOW CONFERENCE
Quebec City 1993

Geometry of Patchy Snowcovers

K. SHOOK, D.M. GRAY
Division of Hydrology
Department of Agricultural and Bioresource Engineering
University of Saskatchewan
Saskatoon, Saskatchewan S7N 0W0 Canada

J.W. POMEROY
National Hydrology Research Institute
Environment Canada
11 Innovation Boulevard
Saskatoon, Saskatchewan S7N 3H5 Canada

ABSTRACT

The influence of the spatial variation in snowcover water equivalent on areal snow-cover depletion and the geometry of snow patches that form during the ablation of shallow, seasonal snowcovers in open environments is discussed. A simplified snowpack ablation simulation is used to demonstrate that the fractal structure of the snowcover water equivalent causes soil and snow patches to possess fractal characteristics. This program is a distributed, grid-square model that uses a synthetically-generated snowcover and includes an algorithm for approximating the effects of local advection on melt. Fractal dimension(s) of snow patches produced by the model are shown to agree closely with the dimensions of natural ablated snowcovers determined from analyses of aerial photographs.

INTRODUCTION

Information on the temporal variation in snow-covered area of watershed during melt is requisite for accurate predictions of runoff. In open environments, the extent of the gross area of a watershed that is snow-covered affects runoff primarily in two ways: (a) it influences the melt rate, because patches of bare ground affect the energy balance of the snow field, and (b) it governs the contributing area of runoff. The highest rate of meltwater production on a watershed will occur when the product of the average melt rate and snow-covered area is a maximum.

Large areas of bare ground within a snow field significantly alter its energy balance. Bare ground, having a lower albedo than snow, absorbs larger amounts of solar radiation and heats more quickly. Local advection of energy from the bare patches and the turbulent transfer of latent and sensible heat to adjacent snow surfaces increase the melt rate. Melting due to advection is most noticeable along the edges of snow patches. Small snow patches are dominated by turbulent melt throughout the season, or until they disappear; larger snow fields are dominated by radiation melt early in the season and turbulent melt late in the season as they decrease in area.

For a specific melt rate, less meltwater is generated over a watershed when it is partly snow-covered than if completely-covered. Erickson et al. (1978) reported strong correlations between daily snowmelt runoff, mean daily air temperature and extent of snowcover on small watersheds in the Canadian prairies. Martinec and Rango (1986), warn against compensating a meltwater difference that arises from erroneous snowcover information by "optimizing" the melt factor used to calculate snowmelt.

Geometry of Ablating Snowpacks

Shook et al. (1993) applied image analyses to aerial photographs taken during snowmelt on two small watersheds: one located in the Canadian Prairies, the other in the alpine region of the Austrian Alps. They found that the soil and snow patches that form during ablation behave as fractal objects. That is, they have no characteristic size or scale and their quantity of roughness remains constant under increasing magnification. This latter property is know as self-similarity. The perimeter-area and area-frequency characteristics can be

described by power equations (Mandelbrot, 1983):

Perimeter-Area Relationship

$$P = kA^{\frac{D_P}{2}}, \text{ and} \qquad [1]$$

where P = perimeter,
k = constant,
A = area, and
D_P = fractal dimension (values of $D_P > 1.0$).

Korčak's Law

Korčak's law is a rule of thumb that has been found to apply to many fractal systems. The law states that the areas of natural fractal objects will follow a hyperbolic size distribution, i.e.,

$$F(A) = cA^{-\frac{D_K}{2}}, A \geq A_{min}, \qquad [2]$$

where F(A) = fraction of the number of objects with a size equal to or greater than area, A,
c = the area of the smallest resolution cell, and
D_K = fractal dimension.

D_K indexes the degree of concentration of area. A small value indicates that most of the area is concentrated in only a few objects; a large value indicates a more uniform distribution of areas.

On the basis of their findings Shook et al. (1993) concluded: (a) soil and snow patches have the same fractal dimension, and (b) snow patches are not random and their size distribution is predictable. When the fractal dimension is known, the perimeter length and relative frequency of patches of specific size can be estimated by Eqs. 1 and 2. This information is required for assessing the influence of advective energy transfers on melting of patchy snowcovers.

Areal Depletion Curves

An areal-depletion curve is often used to correct quantities of melt and runoff, calculated assuming complete snowcover on a basin, for the fraction of the basin area that is snow-covered. Because areal-depletion is strongly affected by the structure (depth and spatial distribution) of the snowcover water equivalent, SWE, numerous studies have used this parameter as the basis for modelling the process (e.g., U.S. Army Corps of Engineers, 1956; Anderson, 1973; Martinec, 1985). Once the relation between the areal extent and the areal water equivalent of snowcover is known, the fraction of a basin that is snow-covered is approximated from estimates of the amount of melt.

Dunne and Leopold (1978), Ferguson (1984), Buttle and McDonnell, (1987) and Donald (1992), apply one-dimensional melt rates to the distribution of SWE to model the areal extent of snowcover on a basin at various stages of melt. A depletion curve developed in this manner does not include the effects of: (a) local advection on melt, (b) changes in the geometry of the soil and snow patches on the advective component, (c) changes in the albedo of snow due to metamorphism, or (d) changes to the energetics of snowmelt due to the penetration of solar radiation through snow to the underlying ground.

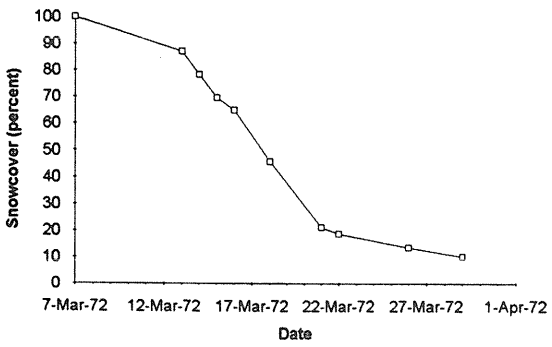

Figure 1. Depletion in snow-covered area on a prairie watershed due to ablation - Smith Tributary, Fiske, SK, 1972.

Figure 1 typifies the depletion in snow-covered area on a prairie watershed due to ablation. The curve has a "sigmoidal" shape in which lower rates of depletion at the beginning and end of melt bound a period when the area of snowcover decreases more rapidly. Figure 2 shows the cumulative frequency curve of snow water equivalent derived from measurements from level fallow and stubble fields in a prairie landscape. Using these data, the important role of the distribution of the water equivalent of a snowcover in areal snowcover depletion can be demonstrated by simple simulation. Figure 3 shows area-depletion curves derived by applying "advanced", "uniform" and "delayed" one-dimensional melt patterns to an array of elements having the distribution of water equivalent given by Fig. 2. Each depletion curve has a sigmoidal shape, independent of melt pattern. Only a few shallow elements (the right side of the frequency distribution) are cleared at the beginning of

simulated melt. The majority of elements are cleared by melting from points whose water equivalent fall within mid-range. A few deep elements (the left side of the frequency distribution) retain snowcover for many intervals. Increasing or decreasing the melt rate shifts (advances or delays) and changes the slope of the curve, but does not alter its basic shape.

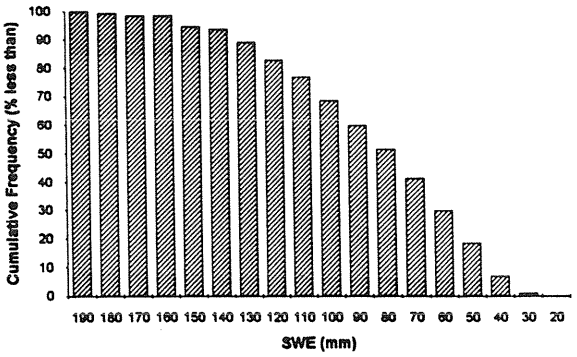

Figure 2. Cumulative frequency distribution of SWE on level fields of fallow and stubble in a prairie landscape, Saskatoon, SK, 1980.

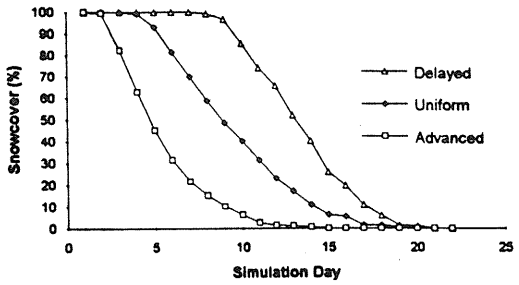

Figure 3. Areal-depletion curves by one-dimensional melt patterns applied to an array with the SWE-distribution in Fig. 2

SPATIAL DISTRIBUTION OF SNOWCOVER WATER EQUIVALENT

An understanding of the development of soil and snow patches of ablating snowcovers as fractals is required for synthesizing the patches in small-scale models of ablation. In this paper it is assumed: (a) the fractal characteristics of soil and snow patches are the result of the spatial variation in the snowcover water equivalent, SWE, and (b) the distribution in SWE is fractal.

There is evidence that the ground surface is generally fractal (Burrough, 1981). Therefore, any completely-uniform bed of material having a smooth surface that covers the ground would be fractal in its thickness. Also, since the surfaces of deposits of wind-transported snow are highly irregular, the SWE is likely to behave as a fractal. Shook (1993) applied the Hurst exponent (Feder, 1988) to test the fractal structure of snow depth. The Hurst exponent, H, reflects the sensitivity of the variation of data from its mean to sample size. It was originally developed to index autocorrelation in data sets. H = ~0.5 suggests the data is random; H>0.5 suggests the data is fractal. Small-scale surveys of snow depth on relatively-flat fields of fallow and wheat stubble in a prairie landscape produced values for H varying from 0.53 to 1.03 (average H = 0.75). On the basis of these findings Shook (1993) concluded that snow depths are generally fractal. Because SWE is directly related to snow depth (by calculation) and because deeper wind-deposited snow is denser snow (Tabler and Schmidt, 1986) it is unlikely that the fractal dimension for water equivalent will differ appreciably from that for depth. This is especially true if the variability in snow density is less than that of snow depth.

That snow depth appears to be fractal at small scales supports the propositions: (a) the formation of natural snow patches during ablation is due to the spatial variation in the water equivalent of a snowcover and (b) the departure of large snow patches from Korčak's law (Shook et al., 1993) is related to scale. At small scales, the fractal structure of the SWE should cause a snowcover to ablate as a fractal object, i.e., retain its' self-similarity. If the fractal character of snow depth is a property of the snowcover, and poorly-related to large-scale differences in topography of the underlying land surface, this would explain why snowcovers in widely-different landscapes show similar behaviours. Large scales, dominated by landscape topography, form snowcovers that may be fractal, may only be fractal at larger scales, or may have a different fractal dimension. The larger soil and snow patches produced by these large-scale effects will therefore behave differently from the smaller patches.

MODELLING SNOWPACK ABLATION

Simplified Model

A Simplified Snowpack Ablation Simulation, SSAS, was developed to model snowcover ablation. The objective of SSAS is to reproduce the geometry of natural soil and snow patches by using

approximations of the actual energy transfer functions.

SSAS is a distributed, grid-square model. Each element in the grid is assigned a predetermined depth and density of snow. Melt fluxes are applied to a model snowpack to cause melting. As areas of bare ground appear, some of the solar energy they absorb is transferred to the atmosphere. As the air moves downwind over fetches of bare soil, additional amounts of energy are transferred until the air reaches the upwind edges of patches of snow. At the leading edges of snow, the direction of the turbulent energy transfers is reversed and heat is added to the snow patches. Because the system incorporates the areal distribution of snowmelt, SSAS is a three dimensional model.

SSAS Algorithms

No scales are used in SSAS because: (a) SSAS is intended to establish the viability of a particular type of modelling and does not represent any particular location; (b) the ablation process appears to be fractal over a large range of scales, therefore the program should be valid for a wide range in size; and (c) the program is intended to produce fractal results, therefore the introduction of artificial characteristic lengths is generally to be avoided.

SSAS is constructed of several modules that are executed linearly during each iteration. The program begins with a completely snow-covered area and iterates until the snowcover is less than one percent of the modelled area. The structure of the program blocks is shown in Fig. 4. The functioning of each block is described below.

Get Run Parameters

The run parameters are input by the program operator at the beginning of each run. Generally, the parameters determine the methods for the construction of the synthetic snowpack and the magnitudes of the melt rates and energy exchanges.

Set-up Arrays

The most important component of the program is the array, **DEPTH**, which contains up to 200 x 200 elements. **DEPTH** holds the values of SWE used by the model. Each array element is mapped to a pixel on the screen, providing a visual display of the melt sequence. If the snow water equivalent of an array element is less than a user-defined threshold, the element is empty of snow and a black pixel will be plotted on the screen. If the value is greater than the threshold, a white pixel is plotted.

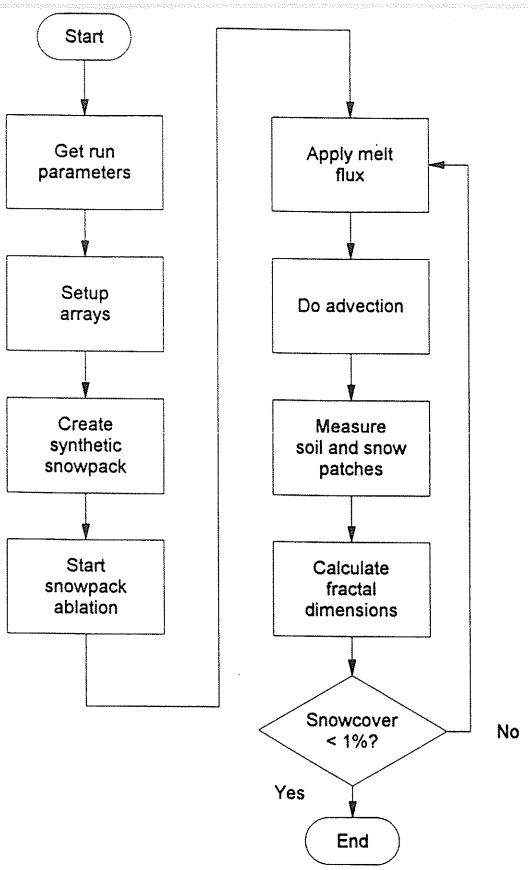

Figure 4. Structure of Simplified Snowpack Ablation Simulation (SSAS) Program.

Create Synthetic Snowpack

A distribution of SWE of a synthetic snowcover is generated using a technique known as the fractal sum of pulses, FSP, which was developed by Lovejoy and Mandelbrot (1985) for modelling clouds and rainfall. Sets of pulses (collections of array elements) are chosen to fit a pre-determined distribution. The dimensions of each pulse are determined by a biased pseudo-random process. According to Lovejoy and Mandelbrot, it is necessary for the pulse sizes and values to be hyperbolically-distributed to generate a fractal object. Each array element in each pulse is assigned a value, again according to a distribution. The values of the pulse elements may be positive or negative. The pulses are then placed at a random location within the final array. As each pulse is placed within the array, the value of the pulse is added to the previous value of the array element. The process is repeated for the desired number of pulses.

The FSP process used to synthesize a snowcover placed "cylinders", i.e., round collections of array

elements, in the array. Shook (1993) gives a program listing for this algorithm. Several parameters are requested from the user to generate the FSP surface. They include: the number of circular pulses, the maximum pulse radius permitted, the exponent for the hyperbolic diameter and depth relationships and the cylinder aspect ratio (of cylinder height to radius). As demonstrated in later discussions, snowpacks generated by this procedure possess fractal properties.

Start Snowpack Ablation

Snowpack ablation is an iterative process. In each iteration the simulated snowpack is subjected to melt fluxes and the resulting soil and snow patches are measured. No attempt is made to measure the soil patches until at least 1% of the model area is snow-free.

Apply Melt Flux

The melt flux is assumed constant for each time step. A constant "depth" of melt (input by the user) is subtracted from all elements whose "depth" is greater than zero, at each iteration of the program.

Do Advection

If the SWE of an element is zero, it is assumed that a portion of the energy flux it receives will be used as sensible heat, which in turn, will be transported downwind by the atmosphere and advected to an adjacent snow patch. The amount of energy available for local advection is simulated by multiplying the melt flux by a user-specified factor. Only part of this energy is transferred and the fraction is specified by the user in terms of the number of array elements that are designated as required for the transfer of the total energy available for advection from one element. That is, if the user specifies 5 elements as the length required to effect the transfer of 100% of the energy available, then each bare element will contribute 1/5 of its available supply. Therefore, the longer the fetch (up to the maximum specified by the user), the greater the quantity of energy advected. The simulated energy transfer is linear, whereas the actual process is nonlinear (Weisman, 1977).

SSAS assumes that wind occurs only in the direction of the four main compass points. In each time step, the wind direction is constant and air moves once across the array. This may cause a characteristic length in that the time step is related by the wind velocity to the travel distance.

When the simulated wind reaches an array element containing snow, the energy contained in the air is transferred to the snowpack and reduces its water equivalent by a corresponding amount of melt. Advective energy is distributed uniformly over the snow fetch.

Measure Soil and Snow Patches

The primary output of SSAS is the display of the array **DEPTH** that is mapped to the screen. Displaying the appearance of the snowpack provides the operator a visual display by which to judge the realism of the simulation. Analysis of the patch geometry requires the measurements of the perimeters and areas of the patches and the calculation of the fractal dimensions, D_P and D_K.

The perimeter of each patch is measured with a "bug", a small array (2x2 elements) that "walks" around the outside of the patch by examining the geometry of the edge of the patch. The principle of using a bug to trace an irregular outline is well-known in image processing applications (Rosenfeld and Kak, 1982). As the bug walks around the edge of the patch, it counts the number of elements in the patch perimeter and the location of each edge element. When the bug returns to its original starting point, the tracing of the patch is complete.

Measuring the area involves determinations of the maximum and minimum array columns of each array line of the patch. The area of the patch is determined by counting the number of patch elements on each line between the maximum and minimum array columns.

Calculate Fractal Dimensions

The patch perimeters and areas are stored in separate arrays as they are determined. When all patches have been found, the fractal dimensions, D_P and D_K, are calculated. The perimeter, area and F(A) are transformed into their logarithmic values and least-squares lines fitted to the transformed data following procedures described by Press et al. (1986).

The iterations of snow ablation are repeated until 99% of the model area is snow-free. This threshold was set to prevent errors that would have been generated if the program had tried to measure non-existent snow patches.

RESULTS OF ABLATION SIMULATION

Figure 5 plots normalized values of the perimeters and areas for snow patches: (a) generated by the model (SSAS), (b) determined from image analyses of aerial photographs of a field of summer

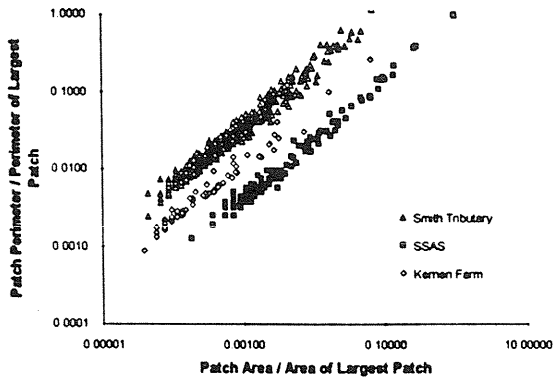

Figure 5. Normalized perimeter-area relationships for snow patches from SSAS, fallow field and Smith Tributary with ~50% snowcover.

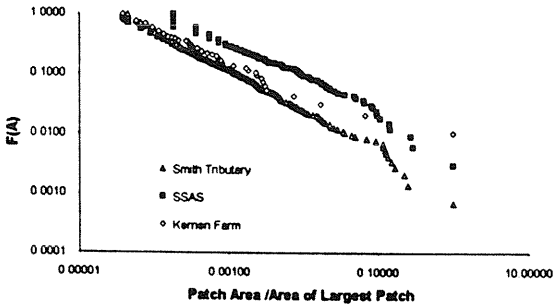

Figure 6. Normalized area-frequency relationships for snow patches from SSAS, fallow field and Smith Tributary with ~50% snowcover.

fallow and (c) determined from analyses of aerial mosaics of a small watershed in western Saskatchewan (Smith Tributary). Figure 6 shows corresponding normalized plots of the size - frequency distribution for modelled and natural patches. These data represent the case when the respective arreas are about 50% snow-covered.

An appreciation of the differences in topography of the fallow field and Smith Tributary can be obtained from Figs. 7 and 8. The fallow field is a relatively-flat, 4.5-ha parcel of land that is denuded of vegetation. Smith Tributary is a catchment with a surface drainage area of about 1.9 km^2. Its main drainageways are deeply-incised and are subject to preferential accumulation of wind-transported snow. The primary vegetation on the channel slopes are Prairie grass and shrubs. The watershed drains an upland area of flat and gently-moderately rollingtopography that is under cultivation for the production of cereal grains by dryland farming

Figure 7. Aerial photograph of fallow field at Kernen Farm, Saskatoon, SK.

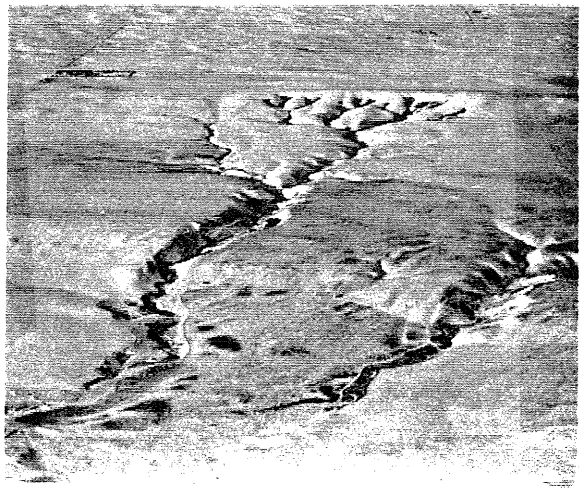

Figure 8. Aerial photograph of Smith Tributary, Fiske, SK.

practices.

The data in Figs. 5 and 6 show that the perimeter-area and size-distribution characteristics of the modelled and natural snowcovers exhibit similar trends. For example, the perimeter - area relationships are linear over a wide range of patch size and the size distributions of small patches generally follow Korčak's law whereas the larger patches depart from the linear association. Note: displacements of the curves in the vertical and horizontal directions are due to differences in the perimeter and the area of the largest patch used to normalize the plots for the various cases.

The fractal dimensions (Eqs. 1 and 2) of snow patches produced by the model and those monitored on the fallow field and the Smith Tributary are

listed in Table 1. As expected, since the model and the fallow field are essentially flat planes, there is closer agreement in the dimensions of the patches of these units than in the dimensions of patches for the model and Smith Tributary. The larger values of D_p and D_K for the catchment indicate: (a) the edges of the patches are rougher, i.e., for a patch of given size the perimeter length is longer, and (b) the distribution of areas of patches is more uniform.

Table 1. Fractal dimensions of model and natural snowcovers.

Unit	*Fractal Dimensions*	
	D_P	D_K
Model (SSAS)	1.46	1.13
Fallow Field	1.46	1.20
Smith Tributary	1.58	1.32

Nevertheless, the agreement in fractal dimensions for model and catchment snow patches is exceptional considering: (a) the model parameters were not optimized to "best" fit the natural data, (b) the large dissimilarities in topography, vegetation and other landscape features of model and prototype systems, and (c) the effects of differences in hydrological processes, e.g. melt rates and advection, are ignored. Shook (1993) discusses a number of other factors that may have contributed to the differences such as: method of measuring patch geometry, size of model snowpack, measurement precision of image analyses system and quality of aerial photographs. On the basis of these results it is suggested that the areal-depletion of snowcover and the geometry of snow patches that form during ablation are primarily due to the frequency distribution and fractal structure of the snow water equivalent.

SUMMARY

The areal depletion of snowcover during ablation in an open prairie environment is strongly affected by the spatial variation in the water equivalent of a snowcover. To demonstrate the effect, a one-dimensional melt model is applied to an array of elements in which the water equivalent is assigned the frequency distribution of natural snowcover. The general shape of "simulated" depletion curve(s) closely parallel the profile of areal depletion of snowcover monitored in the field.

Evidence is provided which suggests that at small scales the spatial distribution of the water equivalent of a snowcover is fractal. It is assumed that it is the fractal structure of the water equivalent that causes soil and snow patches to possess fractal characteristics. This assumption is verified by comparing the fractal dimension(s) of snow patches produced by a simplified ablation simulation, SSAS, to the dimensions of patches monitored on a relatively flat field of fallow and on a small watershed. The program, SSAS, is described. It is a distributed, grid-square model that includes an algorithm for approximating the effects of local advection on melt and uses synthetic snow data generated by a technique known as the fractal sum of pulses. The fractal dimensions calculated from the perimeter-area relationships of the patches for the model, fallow field and watershed were 1.46, 1.46 and 1.58 respectively; the dimensions calculated from the size-frequency characteristics of the patches were 1.13, 1.20 and 1.32 respectively.

LITERATURE CITED

Anderson, E.A., 1973. National weather service river forecast system - snow accumulation and. ablation model. NOAA Tech. Memo. NWS HYDRO-17, U.S. Dept. Commer., Washington, D.C.

Burrough, P.A., 1981. Fractal dimensions of landscapes and other environmental data. Nature 294:240-242.

Buttle, J.M. and J.J. McDonnell, 1987. Modelling the areal depletion of snowcover in a forested catchment. J. Hydrol. 90:43-60.

Donald, J.R. 1992. Snowcover depletion curves and satellite snowcover estimates for snowmelt runoff modelling. Ph.D Thesis, Univ. Waterloo, Waterloo, ON, 232 pp.

Dunne, T. and L.B. Leopold, 1978. Water in Environmental Planning. Freeman, San Francisco, CA.

Erickson, D.E.L., W. Lin and H. Steppuhn, 1978. Indices for estimating Prairie runoff from snowmelt. Pap. presented to Seventh Symp. Water Studies Institute, Applied Prairie Hydrol., Saskatoon, SK.

Feder, J., 1988. Fractals. Plenum Press, New York, NY.

Ferguson, R.J., 1984. Magnitude and modelling of snowmelt in the Cairngorm mountains. Hydrol. Sci. J. 29:49-62.

Lovejoy, S. and B.B. Mandelbrot, 1985. Fractal

SNOW CLIMATOLOGY OF THE NORTHEASTERN UNITED STATES

Median annual snowfall in the northeastern United States ranges from less than 50 cm in eastern Maryland and Delaware to over 250 cm at high elevations and in the snowbelt areas of the Great Lakes (Cember and Wilks 1993). Snow cover is sporadic and shallow in the southern coastal region, but is persistent and lasts for 120 days or longer in the north. Even in the north, where snow cover persists through the winter, maximum temperatures above 0°C typically occur on 5 to 10 days in both January and February and periods of melt may occur anytime (Schmidlin et al. 1987). Median annual maximum snow depth is 10 cm in the south but exceeds 70 cm in the north and mountains (Cember and Wilks, 1993). Extreme depths for the full record exceed 100 cm in the north and the Great Lakes snowbelts.

MEASUREMENT OF SWE

The measurement of SWE by the National Weather Service is usually taken over sod a few meters from the NWS office on the grounds of large airports. These are flat, open landscapes and may not be representative of SWE in the general region (Schmidlin 1989, 1990). Some NWS offices take SWE observations on a roof, cultivated field, gravel lot, or in nearby wooded terrain (Schmidlin, 1990). Data are recorded and published in inches so those units have been preserved here. Time of measurement of SWE is 1800 UTC while snow depth is measured at 1200 UTC (NCDC 1989). The SWE may be obtained by one of three methods at NWS offices -melting, weighing, or estimation (U.S. Department of Commerce 1982). The melting method requires one core of snow to be obtained from a representative location, usually with the 20 cm diameter precipitation gauge. The core is taken inside, melted, and the depth of water in the snow core is obtained. In the weighing method, a core is taken and the core and coring device are weighed to obtain the SWE. Estimation, often assuming a 10:1 snow:water ratio, is used if severe weather conditions prevent the observer from taking a core sample, although one NWS office weighed a core every Monday but estimated SWE on other days (Schmidlin, 1990). The measurement method varies with NWS office protocol and observer preference. Information on the measurement method is not preserved with the data.

THE QUALITY CONTROL MODEL

The quality control procedure described here is an automated process to identify daily SWE measurements that are unreasonable in relation to the previous day's measurement, observed precipitation, or melt (Fig. 1). We start with the assumption that the measurement of SWE is correct. Observations of SWE and other elements at NWS offices are taken by full-time NWS employees. This is in contrast to the 8300 stations in the Cooperative Observer Network where observations are taken by 'citizen volunteers' with less training and supervision. Most of the effort at quality control at the National Climatic Data Center has focused on these Cooperative stations (Reek and Crowe 1991; Reek et al. 1992) where snow data are particularly poor (Robinson 1989; T. Reek, communication 1992).

Two tactics are commonly used in climatological quality control; (1) comparisons with nearby stations to detect inconsistencies, or (2) a scheme that determines whether a datum is outside of reasonable ranges or does not logically follow with observations from adjacent periods (Brandow and Lourick, 1991; Heim et al. 1991; Reek et al. 1992; Robinson, 1993). The former is not practical with

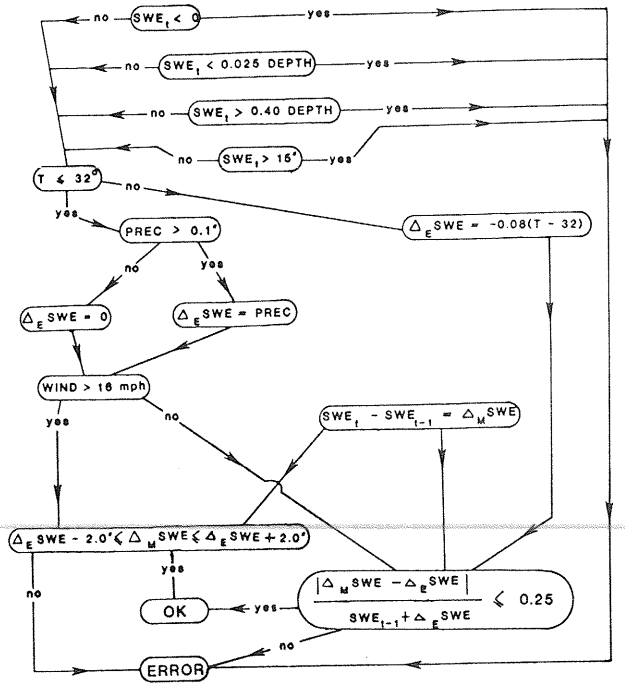

Figure 1. The SWE quality control model. Subscript 't' is today, 'E' is estimated, and 'M' is measured. Variables are defined in the text.

SWE because NWS offices are too far apart (100-300 km) for reliable comparisons among neighboring stations. Therefore, the second tactic is used here.

Errors in daily SWE may be digitizing errors or observer errors. Examples of digitizing errors are a misplaced decimal, an added digit, and reversal of sign or digits in the initial recording or during data entry at the National Climate Data Center. Observer errors include incorrect measurements, due, for example, to careless reading of gauges or incorrect melting of a snow core. Estimation of SWE for several days, possibly introducing errors, followed by a measurement that abruptly incorporates several days of change in SWE may also give an anomalous SWE. This quality control procedure is designed to identify such problems in the data. A daily SWE observation is concluded to be a potential error if it is inconsistent with the previous day's SWE, recorded precipitation, estimated melt, or potential changes due to wind drifting.

A daily increase of SWE should equal the water equivalent of new precipitation during periods of accumulation minus water lost from the snowpack. The water content of snowfall is recorded hourly as precipitation. A daily decrease in SWE during thaw should equal the melt and runoff from the snow. Although snow depth is measured daily, a decrease in depth cannot be interpreted as melt and loss of water from the snowpack because compaction may occur within the snowpack without loss of water. Therefore, loss of water through melt must be estimated from other measured elements, such as temperature. SWE may also increase or decrease due to phase changes by exchange directly with vapor in the atmosphere. Goodison (1979) showed daily sublimation from snow in southern Ontario was typically 0.1 mm to 0.3 mm of water equivalent. Daily sublimation or condensation onto the snowpack are considered insignificant with respect to the 0.1 inch (2.5 mm) precision in SWE measurement and are probably compensating over several days (Wilson 1954). Strong winds during snowfall may cause daily changes in SWE that are inconsistent with daily precipitation during snow storms. Wind drifting may also cause a change in SWE in the absence of precipitation or melt. The daily measurement of SWE may also vary without new snowfall, melt, or drifting, due to the natural small- scale spatial variability of snow covers. An acceptable range is established in the quality control procedure for this natural variability. Limit checks and ranges of acceptable anomalies in SWE from consistency with the previous day's observation, precipitation, melt, and wind, are described in the following sections.

Digitizing errors and limits checks

Each datum is initially checked for the most likely digitizing errors and for exceeding reasonable limits with respect to the local climate (Fig. 1). SWE less than zero is flagged as an error caused by an added negative sign. SWE less than (0.025 x snow depth) is flagged as a potential error since snowfall/SWE ratios greater than 40:1 are unlikely at temperatures above 0°F (Reek et al 1992). SWE greater than (0.40 x snow depth) for two consecutive days is flagged as a potential error because these high densities are rarely encountered in the eastern United States (Edgell 1988). Two consecutive days of depth must be examined and compared to SWE because the 6 hr lag between the daily observations of snow depth and SWE may allow significant SWE to accumulate after the daily observation of snow depth. SWE greater than 15 inches (38 cm) is also flagged as a potential error. This is the maximum SWE at Caribou, Maine (Loiselle et al. 1992), generally the NWS office with the greatest annual SWE in the northeast. Daily SWE measurements that pass these tests proceed to checks for consistency with previous day's SWE, melt, precipitation, wind, and natural spatial variability of SWE.

Snow Melt

There are many schemes to estimate daily snowmelt from weather data (Male and Gray 1981; Bloschl and Kirnbauer 1991; Hughes and Robinson 1993). Most require complex energy balance calculations and are not suitable for this quality control process. Simple models of snowmelt have used air temperature as an index of melt. A base melt threshold air temperature of 0°C is a common assumption (Male and Gray 1981) although other melt thresholds are reported depending on terrain, climate, and vegetation (Carr 1988; Samelson and Wilks 1993). Carr (1988) tested several relationships and found (1),

$$M = 0.08\,(T - 32) \qquad (1)$$

where M is daily SWE decrease in inches day^{-1} and T is mean daily temperature (°F), performed best in southern Ontario. This snowmelt model is simple in its use of one readily available parameter. In this quality control procedure, (1) is used to estimate daily loss of SWE due to snowmelt. Mean

temperature is taken as the average of the high and low temperature on the day of SWE measurement. For a day with mean temperature over 32°F (0°C), the expected daily decrease in SWE equals M in (1).

New Precipitation

SWE may increase by new snowfall or rain into the snow cover, if runoff does not result. New snowfall should result in an increase in SWE that is equal to the water equivalent of the new snowfall. Snowfall is measured and recorded by the NWS as hourly precipitation by weighing or melting snow that fell into the precipitation gauge or by taking one core of new snow that fell onto a snow board placed on top of the previous day's snow cover. The water equivalent of new snowfall is difficult to measure because snow does not readily fall into precipitation gauges and drifting may give large spatial variability in new snow cover, as discussed below. On days with precipitation over 0.1 inch (0.25 cm) water equivalent and mean daily temperature 32°F (0°C) or below, the expected daily increase in SWE is equal to precipitation in the 24 hr ending at 1800 UTC.

Wind Effects

Falling snow is distributed on the landscape as a function of wind speed and roughness features in the landscape. Light winds without blowing snow give a relatively even spatial distribution of depth, density, and SWE, while stronger winds cause blowing snow and result in an uneven pattern of scouring and drifts. Strong winds may also cause redistribution of an existing snow cover. Snow transport by wind is greatest over flat, extensive areas, free from obstructions to the airflow (McKay and Gray 1981). The airport sites where SWE is measured at NWS offices match this description and have the potential for considerable drifting snow.

Discrepancies between new snowfall (or lack thereof) and daily changes in SWE may sometimes be explained by effects of wind on the snow cover. Wind speed measured at 10 m height (or corrected to that height) at the NWS offices was incorporated into the model. The model does not estimate the depth of SWE added or removed by wind, because this is micro-site specific, but a minimum threshold wind speed for drifting snow was established. Winds above this threshold were assumed to have the potential to redistribute the snow cover and cause anomalous changes in SWE.

The relationship between threshold wind speeds and snow characteristics is complex (Schmidt 1980) but generalizations are available for this application. Kind (1981) showed that a 10 m wind speed of 5 ms^{-1} (11 mph) is the minimum threshold to cause drifting snow if the snow is loose, fresh, and dry, and a threshold wind speed of 11 ms^{-1} (25 mph) for drifting of old, hardened snow. Pomeroy and Gray (1990) recommended a minimum threshold 10 m wind speed of 7 ms^{-1} (16 mph) to cause drifting of typical snow covers on non-vegetated plains. This value was adopted as the threshold for this model.

The increase of wind speed with height depends on surface roughness and atmospheric stability. It is approximated by the power law in (2), where U_{10} is the wind speed at 10 m, U_z is the wind speed measured at height z, d is snow depth, and 'a' is an

$$U_{10} = U_z[(10-d)/(z-d)]^a \qquad (2)$$

exponent representing all friction components (Landsberg 1981, p. 140). The value of 'a' is relatively low over open, flat surfaces. For open terrain, it has been given as 0.14 to 0.18 by Landsberg (1981, p. 140-141) and 0.125 by Sissenwine and Cormier (1974). A value of 0.125 for 'a' was adopted to convert wind speeds measured at NWS offices to a standard 10 m height.

Hourly wind speeds were checked for each 24 hr period ending with the 1800 UTC SWE observation time on days with a mean temperature of 32°F (0°C) or below. Snow covers on days with mean temperature over 32°F (0°C) were assumed to be melting and less vulnerable to drifting. If an hourly wind speed over 16 mph (7 ms^{-1}) was recorded on a sub- freezing day, then we assume that inconsistencies of up to 2 inches (5 cm) between the measured daily change in SWE and the 'expected' daily change of SWE, based on new precipitation or melt, could have resulted from drifting. Inconsistencies greater than 2 inches are flagged as potential errors. If no hourly wind speed over 16 mph (7 ms^{-1}) occurred, then further checks were made for consistency with micro-scale variability of SWE.

Micro-scale spatial variability of SWE

The SWE cannot be measured at exactly the same location each day because it requires a destructive sampling process. In general, the daily snow cores are taken less than 10 m apart at a site adjacent to the precipitation gauges at NWS offices. Some

micro-scale variability in snow depth and density, and therefore SWE, is expected within this area, even in the homogeneous terrain of airports. Variability in snowcover at the micro-scale is due to numerous interactions, principally between surface roughness and transport phenomena (McKay and Gray 1981). Goodison (1979) showed open areas of short grass have the most variable snow cover of several land use types in southern Ontario. SWE has more variability than snow depth across a landscape (Wilson 1954). Therefore, some daily variability in measured SWE at NWS offices is expected even if actual SWE does not change and the measurement is taken properly.

Literature on spatial variability of SWE has focused on snow courses, with point measurements tens of meters apart along a linear transect in forested terrain (for examples, Wilson 1954; Leaf and Kovner 1972; Brandow and Lourick, 1991). To assess micro-scale variability in SWE, field experiments on SWE were conducted during the winter 1992-93 over small uniform areas, similar to the SWE sampling sites at airports. Seven plots were sampled to measure the intrinsic variability of the SWE measurement. Two plots with nine points 2 m apart on a square grid were sampled near Kent, OH. Five plots with 8 to 12 points spaced 1 m apart on linear transects were sampled near Ithaca, NY. Each SWE value was determined by melting snow cores and measuring the liquid equivalent using a raingage (U.S. Department of Commerce, 1982). Table 1 shows the dates, locations, sample sizes, snow depth, and SWE data for each of the seven measurement groups. Dates were chosen to exclude snowpacks substantially affected by drifting. Figure 2 shows the standard deviation of SWE and the average SWE for each of the seven sets of measurements. Also shown in Figure 2 are the 95% confidence limits for the average and standard deviation of the SWE.

It is clear from Figure 2 that the intrinsic variability of the SWE measurement increases with the water content of the snowpack. The standard deviation appears to increase approximately in proportion to the mean, so that the coefficient of variation (CV = standard deviation/mean) is approximately constant. Also shown in Figure 2 is the line for CV = 0.125, which is within or above the 95% confidence intervals for the standard deviations in each measurement set. This result agrees with the estimate by Tom Carroll (communication) that ground-based SWE measurements tend to have CV's of 0.10 to 0.20.

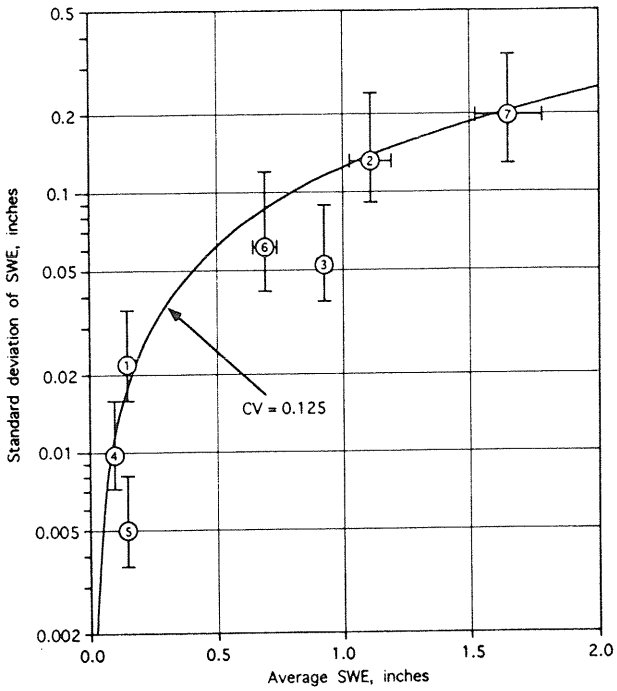

Figure 2. Mean and standard deviation of SWE over level, open sod for samples shown in Table 1. The 95% error bars are shown when possible and the 0.125 coefficient of variation (CV) curve is shown to enclose most points.

Table 1. Measured micro-scale variability in snow depth and SWE over level sod in open terrain.

Date	Location	n	Depth (in)		SWE (in)	
			mean	std dev	mean	std dev
8 Dec 1992	Ithaca, NY	15	2.9	0.46	0.14	0.02
12 Dec 1992	Ithaca, NY	10	5.8	0.89	1.11	0.13
14 Dec 1992	Ithaca, NY	12	4.9	0.50	0.92	0.05
11 Jan 1993	Ithaca, NY	15	2.2	0.21	0.10	0.01
12 Jan 1993	Ithaca, NY	13	1.8	0.28	0.14	0.01
17 Feb 1993	Kent, OH	9	5.4	0.19	0.69	0.06
3 Mar 1993	Burton, OH	9	6.9	0.49	1.65	0.20

We conclude that natural variability of SWE over small areas may account for deviations of 25% of the SWE (+/- 2σ), even if great care is taken with the SWE measurement. With wind speeds up to 16 mph (7 ms^{-1}), inconsistencies between measured daily change in SWE and the expected change in SWE, based on precipitation and melt, are accepted if they are no more than 25% of the expected new SWE. Inconsistencies greater than 25% are flagged as potential errors.

SUMMARY

The quality control model shown in Figure 1 for the historical archive of daily SWE measurement at NWS offices provides internal consistency checks, beginning with limits and digitizing checks. Data that pass these move to checks of consistency with daily melt, precipitation, and wind. At mean daily temperatures of 32°F (0°C) or below, SWE should not change beyond limits set except with precipitation. New precipitation under those conditions should be close to the daily increase in SWE. At mean daily temperatures above 32°F (0°C), melt estimated by (1) should be close to the daily decrease in SWE. Wind speeds greater than 16 mph (7 ms^{-1}) at 10 m height may cause drifting that accounts for inconsistencies in SWE of up to 2 inches (5 cm). Micro-scale spatial variability of SWE may account for differences of up to 25% between the observed daily change in SWE and estimated daily change in SWE, based on melt or precipitation. SWE measurements that fail any of these checks are flagged as potential errors for human inspection and possible correction. If a potential error in SWE is noted in the automated procedure, then subsequent days are compared to the last correct SWE measurement, rather than to the erroneous datum. As the model is tested, revisions will be made to limits and other checks and the procedure in Figure 1 will be amended as necessary.

ACKNOWLEDGMENTS

Appreciation is extended to David Robinson, Megan McKay, and an anonymous reviewer for suggestions to improve the manuscript. This research was supported by the Northeast Regional Climate Center under NOAA grant NA16CP-0220-02.

REFERENCES

ASCE, 1990: Minimum design loads for buildings and other structures. ANSI/ASCE 7-88, American Society of Civil Engineers 94 pp.

Bloschl, G. and R. Kirnbauer, 1991: Point snowmelt models with different degrees of complexity - internal processes. J. Hydrol. 129, 127-147.

Brandow, C., and A. Lourick, 1991: Snow sensor data quality indexing. Proc. of the 59th Western Snow Conf., Juneau, 130-133.

Carr, D.A., 1988: Snowpack modeling using daily climatological data. Proc. of the 45th Eastern Snow Conf., Lake Placid, 176-180.

Cember, R.P., and D.S. Wilks, 1993: Climatological atlas of snowfall and snow depth for the northeastern United States and southeastern Canada. Publication No. RR 93-1, Northeast Regional Climate Center Research Series, Cornell University, Ithaca, NY.

Edgell, D.J., 1988: An analysis of the snow water equivalent measurement in Ohio with applications for snowmelt climatology. M.A. thesis, Kent State University, 158 pp.

Ellingwood, B., and R. Redfield, 1983: Ground snow loads for structural design. J. Struct. Div. Amer. Soc. Civ. Eng., 109, 950-964.

Goodison, B.E., 1979: Comparability of snowfall and snow cover data in a southern Ontario basin. In Modeling of Snow Cover Runoff, S.C. Colbeck and M. Ray, eds. (p. 34- 43), Special Report 79-36, USACRREL, Hanover, NH.

Heim Jr., R.R., R.G. Quayle, T.R. Karl, and D. Ezell, 1991; Quality control of monthly data for global climate perspectives. Preprints, Seventh Conf. Appl. Meteorol., Salt Lake City, Amer. Meteorol. Soc., 146-150.

Hughes, M.G. and D.A. Robinson, 1993: Creating temporally complete snow cover records using a new method for modeling snow depth changes. Proceedings of Snow Watch '92 (in press).

Kind, R.J., 1981: Snow drifting. In Handbook of Snow: Principles, Processes, Management, and

Use, D.M. Gray and D.H. Male, Eds., p. 338-359, Pergamon Press, Toronto.

Landsberg, H.E., 1981: The Urban Climate. Academic Press, New York, 275 pp.

Leaf, C.F. and J.F. Kovner, 1972: Sampling requirements for area water equivalent estimates in forested subalpine watersheds. Water Resour. Res., 8, 713-716.

Loiselle, M.C., D.J. Cowing, and G.R. Keezer, 1992: Preliminary analysis of historical snow data using a geographic information system. Proc. of the 49th Eastern Snow Conf., Oswego, 81-88.

Male, D.H. and D.M. Gray, 1981: Snowcover ablation and runoff. In Handbook of Snow: Principles, Processes, Management, and Use, D.M. Gray and D.H. Male, eds., p. 360-436, Pergamon Press, Toronto, 776 pp.

McKay, G.A., and D.M. Gray, 1981: The distribution of snow cover. In Handbook of Snow: Principles, Processes, Management, and Use, D.M. Gray and D.H. Male, eds., p. 153-190, Pergamon Press, Toronto, 776 pp.

NCDC, 1989: Summary of the Day, First Order, TD-3210. National Climatic Data Center, NOAA, 30 pp.

Newark, M.J., L.E. Welsh, R.J. Morris, and W.V. Dnes, 1989: Revised ground snow loads for the 1990 National Building Code of Canada. Can. J. Civ. Eng., 16, 267-278.

O'Rourke, M.J., and U. Stiefel, 1983: Roof snow loads for structural design. J. Struct. Eng., 109, 1527-1537.

Pomeroy, J.W., and D.M. Gray, 1990: Saltation of snow. Water Resour. Res., 26, 1583-1594.

Reek, T., and M. Crowe, 1991; Advances in quality control technology at the National Climatic Data Center. Preprints, Seventh Intl. Conf. on Interactive Info. and Processing Sys. for Meteorol. Oceanogr. and Hydrol., New Orleans, Amer. Meteorol. Soc., 397-403.

Reek, T., S.R. Doty, and T.W. Owen, 1992: A deterministic approach to the validation of historical daily temperature and precipitation data from the cooperative network. Bull. Amer. Meteor. Soc., 73, 753-762.

Robinson, D.A., 1989: Evaluation of the collection, archiving, and publication of daily snow data in the United States. Phys. Geog., 10, 120-130.

Robinson, D.A., 1993: Historical daily climatic data for the United States. Preprints of the Eighth Conference on Applied Climatology, American Meteorological Society, Boston, 264-269.

Samelson, D., and D.S. Wilks, 1993: A simple method for specifying snowpack water equivalent in the northeastern United States. J. Appl. Meteorol., 32:965-974.

Schmidlin, T.W., 1989: Assessment of NWS surface-measured snow water equivalent data based on remotely- sensed data in the northern Plains. Proc. of the 46th Eastern Snow Conf., Quebec, 208-212.

Schmidlin, T.W., 1990: A critique of the climatic record of water equivalent of snow on the ground in the United States. J. Appl. Meteor., 29, 1136-1141.

Schmidlin, T.W., B.E. Dethier, and K.L. Eggleston, 1987: Freeze-thaw days in the northeastern United States. J. Appl. Meteor., 26, 142- 155.

Schmidlin, T.W., D.J. Edgell, and M.A. Delaney, 1992: Design ground snow loads for Ohio. J. Appl. Meteor., 31, 622-627.

Schmidt, R.A., 1980: Threshold wind-speeds and elastic impact in snow transport. J. Glaciol., 26, 453-467.

Sissenwine, N. and R.V. Cormier, 1974: Synopsis of background material for MIL-SRD-210B, Climatic extremes for military equipment. Report AFCRL-TR-74-0052, Air Force Cambridge Research Laboratories, Bedford, MA.

U.S. Department of Commerce, 1982: Federal Meteorological Handbook No. 1.

Wilson, W.T., 1954: Analysis of winter precipitation observation in the cooperative snow investigations. Mon. Wea. Rev., 82, 183-199.